

RESEARCH ARTICLE

Open Access



Characterization of pigments and binders in a mural painting from the Andean church of San Andrés de Pachama (northernmost of Chile)

Eugenia P. Tomasini^{1,2}, José Cárcamo³, Diana M. Castellanos Rodríguez^{1,2}, Valeria Careaga^{1,2}, Sebastián Gutiérrez³, Carlos Rúa Landa⁴, Marcela Sepúlveda^{3,5}, Fernando Guzman⁶, Magdalena Pereira⁷, Gabriela Siracusano^{2,8} and Marta S. Maier^{1,2,8*} 

Abstract

The Andean church of San Andrés de Pachama is located in the highland of the northernmost of Chile, near the limit with Bolivia and next to the *Ruta de la Plata*. This commercial route contributed in the past to the transport and commerce of various raw materials, such as silver, from the Andean mountains region to the Pacific Ocean coast and then to the European market. The walls inside the church are decorated with paintings from the end of the eighteenth century that reproduce religious motifs together with flowers, fruits, and birds. In this study, micro samples taken from one of the mural paintings have been analysed to acquire information on the artistic materials and the painting technique previous to the restoration of the paintings. Analysis by micro-Raman spectroscopy complemented with scanning electron microscopy–energy dispersive X-ray spectroscopy, attenuated total reflection infrared spectroscopy, X-ray diffraction, and high-performance liquid chromatography with diode-array detection allowed the identification of orpiment, vermilion, indigo, smalt, antlerite, hematite, carmine lake, and wood charcoal as pigments as well as gypsum as the ground layer. Lipidic and proteinaceous materials extracted from the microsamples were identified by gas chromatography coupled to mass spectrometry and indicated the use of a mixture of egg and siccativ oil as binders and *a secco* painting technique involving animal glue as the plaster primer. Smalt and the prized cochineal lake are reported for the first time in an Andean colonial mural painting.

Keywords: Micro-Raman spectroscopy, SEM–EDS, GC–MS, Antlerite, Carminic acid, Egg

Introduction

The village of Pachama is located at 3423 masl in the region of Arica-Parinacota in the northernmost of Chile and is one of various colonial towns founded along the *Ruta de la Plata*, a commercial route used since the sixteenth century for the transport of silver ore, commodities from Castilla and other goods from the Cerro Rico of Potosí to the Pacific Ocean [1, 2]. The church of San

Andrés de Pachama (Fig. 1a) was built in the eighteenth century with adobe brick walls, made with earth, clay, and straw. At the end of this century the walls inside the church were decorated with paintings depicting the figures of various saints and the Virgin of the Rosary. Pachama has an iconographic program intended to christianize the earth fertility rituals. The representations of San Isidro, patron of the farmers, and San Cristóbal, protector of the fruit trees, appear crucial to understand the meaning of the mural paintings. Another antecedent is the abundance of vegetal ornamental elements, together with heads of pumas. These figures were related to the rituals of cattle and earth's fertility. Moreover, the

*Correspondence: maier@qo.fcen.uba.ar

¹ CONICET-Universidad de Buenos Aires, Unidad de Microanálisis y Métodos Físicos en Química Orgánica (UMYMFOR), Pabellón 2, Ciudad Universitaria, C1428EGA Ciudad Autónoma de Buenos Aires, Argentina
Full list of author information is available at the end of the article

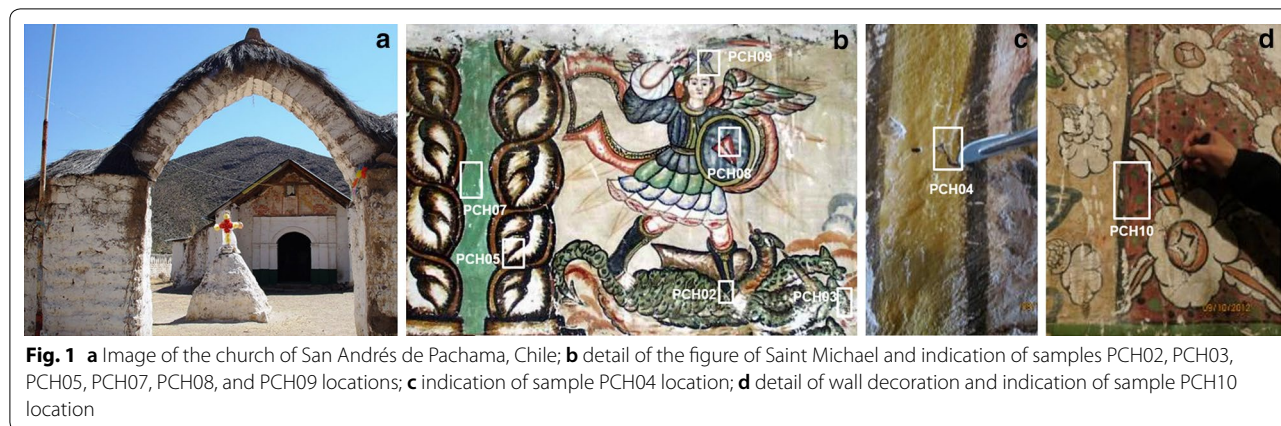


Fig. 1 a Image of the church of San Andrés de Pachama, Chile; b detail of the figure of Saint Michael and indication of samples PCH02, PCH03, PCH05, PCH07, PCH08, and PCH09 locations; c indication of sample PCH04 location; d detail of wall decoration and indication of sample PCH10 location

presence of the images of San Andrés and the Virgin of the Rosary are also significant, since their festivities mark the beginning and the end of the sowing season or pachallampe. Finally, the proximity between the name of the locality and the word Pachamama or Mother Earth is a relevant aspect to be considered [3].

According to its critical state of conservation due to the passage of time and use but also to earthquakes and the humidity caused by the “altiplanic winter”, which causes rains between December and March, the mural paintings showed detachment of polychromy and plaster as well as warpings. The church was restored integrally with funds from the Regional Government, executed by Fundación Altiplano, between January 2016 and January 2017. The restoration proceedings were non-invasive and a lab was installed in situ. For the consolidation or re-adhesion of the polychromy and plasters, “mucilajo”, a mixture of peeled and chopped *Opuntia* cactus in water (with addition of peeled garlic) was used. Only the unstable warpings were treated by injection of a mortar and brick powder, micro-spheres, sodium hexametaphosphate dissolved in water, and “mucilajo”.

Before the restoration, non-invasive analyses performed in situ with a handheld XRF instrument allowed us to obtain preliminar information on the pigments and select the areas of extraction of micro samples of the mural paintings.

The results presented here are part of an ongoing interdisciplinary investigation on the chromatic palette and the technique of execution of relevant mural paintings in Andean churches along the *Ruta de la Plata* [3–5]. In the present study, micro samples from one of the mural paintings of the church of San Andrés de Pachama were analyzed by a combination of micro-Raman spectroscopy, scanning electron microscopy–energy dispersive spectroscopy (SEM–EDS), attenuated total reflection infrared spectroscopy (FTIR-ATR), X-ray diffraction

(XRD), gas chromatography coupled to mass spectrometry (GC–MS), and high-performance liquid chromatography with diode-array detection (HPLC-DAD) in order to determine the chromatic palette and the painting technique. This new information contributes to improve our knowledge on colonial painting techniques used in the Andean region.

Experimental

Samples

Non-invasive measurements on the mural paintings were performed with a handheld XRF Bruker Tracer III-SD instrument in order to obtain preliminar information on the pigments and select the areas of extraction of micro-samples for further laboratory analyses. XRF measurements privileged representative colors of the palette as well as those areas that did not affect the integrity of the painting. Based on this information, eight microsamples (Table 1) were collected with a scalpel from the painting of Saint Michael (Fig. 1b, c) and the flower decoration (Fig. 1d) of the mural. Fragments with an area less than 1 mm² were embedded into an acrylic transparent resin as described in [4]. The cross-sections (Fig. 2) were examined by optical microscopy to obtain information

Table 1 Description of the samples and their location

Sample	Color	Location
PCH02	Dark blue	Saint Michael (boot)
PCH03	Orange	Saint Michael (cloud of fire)
PCH04	Yellow	Saint Michael (sacristy’s arch)
PCH05	Black	Saint Michael (solomonic column)
PCH07	Green	Saint Michael (solomonic column)
PCH08	Red	Saint Michael (shield)
PCH09	Blue	Saint Michael (helmet)
PCH10	Dark red	Wall decoration

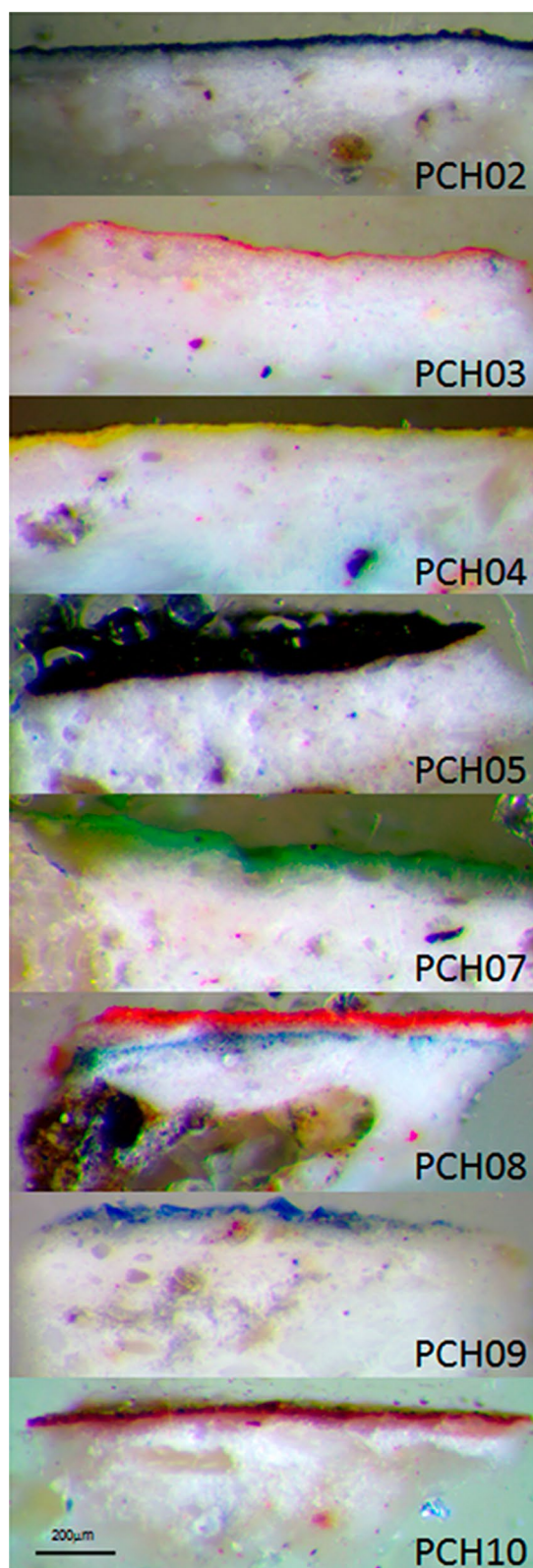


Fig. 2 Optical images ($\times 40$) of the cross-sections of the samples

on the painting and preparation layers and subjected to SEM–EDS and micro-Raman spectroscopy.

A model sample of gypsum was prepared as described previously [4]. Animal glue was applied as a thin layer on the gypsum and dried to constant weight. Then, whole egg was extended on the animal glue layer. After ageing at room temperature for 1 year, a sample was extracted with a spatula and the hydrolyzed proteinaceous fraction was analyzed by GC–MS for comparison purposes.

Instrumentation

Observation and photography of the cross sections of the samples were achieved using a Leica MZ6 stereomicroscope and a Leica DM750 microscope equipped with visible and ultraviolet light sources in the normal and polarized modes. Images were recorded with a Power shot 550 digital cammera.

The cross-sections were coated with platinum and subjected to SEM analyses by secondary electrons (SE) and backscattered electrons (BSE) as described in [4].

Raman spectra of the surface of the samples were obtained with a Renishaw inVia Reflex microscope equipped with a Leica microscope. The resolution was set to 4 cm^{-1} and 1–5 scans of 10–50 s each were averaged for each spectrum. The 785 nm laser line was used and the power was set between 10 and 100 mW to avoid degradation of the sample. Data were collected, analyzed and plotted using the programs WIRE 3.4 and GRAMS 9.0. Raman spectra of the cross-sections were recorded with a DXR Raman microscope (Thermo Fisher Scientific) and a $50\times$ objective. Data were collected using a laser of 780 nm with a 5 cm^{-1} spectral resolution and a laser power below 10 mW at the sample. A confocal aperture of $50\text{-}\mu\text{m}$ slit was used and 80 expositions of 2 s each were averaged.

HPLC–DAD analysis was performed on a Gilson 506C chromatograph as described in [6]. Sample PCH10 and a carmine lake standard (Carmine Naccarat 42100, Kremer) were hydrolysed in acidic methanol as reported previously [7].

For XRD analysis, patterns were measured with a PANalytical Empyrean diffractometer with Cu K α (1.54 \AA) radiation in a Bragg–Brentano geometry. Diffraction patterns were collected from 7 to $60^\circ 2\theta$ with a step size of 0.02° and a recording time of 3 s per step. The small sample was put carefully on alum support and the signal from this support was corrected.

FTIR-ATR spectra of the surface of the collected samples were recorded using a Nicolet iS50 FTIR spectrometer with a diamond single-bounce ATR accessory (Thermo Electron Corp.) in the range of $4000\text{--}400\text{ cm}^{-1}$.

Each spectrum was the average of 64 scans with 4 cm^{-1} resolution.

Analytical methodologies to identify lipidic and proteinaceous binders

In order to detect the presence of organic binders, four painting samples (PCH02, PCH04, PCH05, and PCH08) and the model sample used as reference were extracted with ammonia 2.5 M and chloroform to separate the proteins (ammonia phase) from the neutral lipids (acylglycerides and sterols) in the chloroform phase. This procedure is a modification of the one reported in the literature [8], in particular regarding the extraction of the lipid fraction. Fatty acids were derivatised as their methyl esters (FAME) [9] and analyzed by GC–MS, as described previously [4]. Trimethylsilyl sterol derivatives were prepared and analyzed by GC–MS as reported in [10]. Mass spectra for sterols were measured in the selected ion monitoring (SIM) mode with ions at m/z 129, 329, 368, and 458 for cholesterol.

Amino acids were derivatised as reported previously [11] and analyzed by GC–MS in the electron impact positive mode (70 eV) using a Shimadzu GCMS-QP5050/GC17A (Shimadzu Corporation, Kyoto, Japan) instrument with a ZB-5 (Phenomenex) capillary column (30 m length, 0.25 mm i.d.) coated with (5% phenyl)-dimethylpolysiloxane (film thickness 0.50 μm). Column temperature was increased from 60 to 260 $^{\circ}\text{C}$ at a rate of 25 $^{\circ}\text{C min}^{-1}$ with a 10 min hold at 260 $^{\circ}\text{C}$. The GC inlet temperature was 250 $^{\circ}\text{C}$ (splitless injection) and the MS ion source temperature was 280 $^{\circ}\text{C}$. Mass spectra were run in full scan mode and peak area data were used for quantitation. Amino acids were identified by analysis of mass spectral data and comparison of retention times with amino acid standard (Sigma-Aldrich Co.) derivatives prepared as described in [11].

Results and discussion

Ground layer

Under optical microscopy, the cross-sections of the samples showed two well-differentiated layers attributed to the pictorial layer and a white preparation layer (Fig. 2). The ground layer in the cross-sections of the eight microsamples was analyzed by SEM–EDS (Table 2) and revealed the presence of calcium and sulfur as the main components, as well as silicon. Calcium sulfate with different levels of hydration was detected by micro-Raman spectroscopy with characteristic bands at 418, 501, 611, 627, 676, 1017, 1111, 1130, and 1160 cm^{-1} (Fig. 3). In particular, the stable phases of anhydrite (CaSO_4) (611 and 1160 cm^{-1}), gypsum ($\text{CaSO}_4 \cdot 2\text{H}_2\text{O}$) (1130 cm^{-1}), and bassanite ($\text{CaSO}_4 \cdot 0.5\text{H}_2\text{O}$) (627 and 1017 cm^{-1}) were identified [12]. In addition, two major bands at 1309 and 1394 cm^{-1} , together with minor bands at 1470, 1690, and 1773 cm^{-1} , were associated with degraded organic

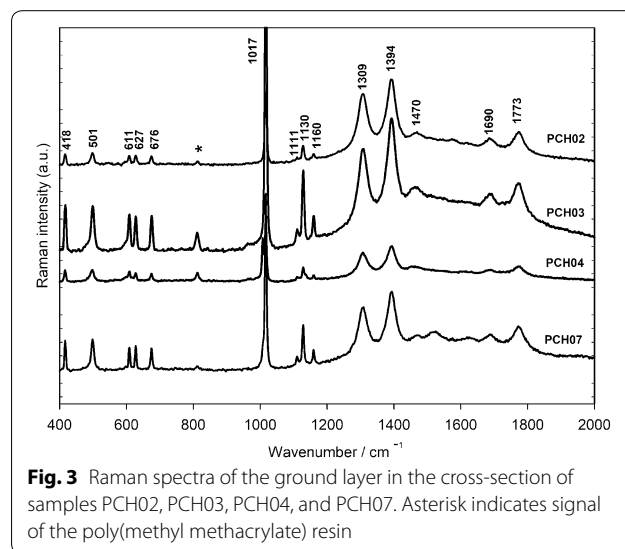


Fig. 3 Raman spectra of the ground layer in the cross-section of samples PCH02, PCH03, PCH04, and PCH07. Asterisk indicates signal of the poly(methyl methacrylate) resin

Table 2 Elemental composition of the surface and cross-sections of the mural painting samples as determined by SEM–EDS

Sample (color)	Surface	Cross-section	
		Pigment layer	Ground layer
PCH02 (dark blue)	<i>Ca, S, Si, Al, Mg</i>	<i>Ca, S, Si, Al</i>	<i>Ca, S, Si</i>
PCH03 (orange)	<i>Ca, S, Si, Al, As, K, Fe</i>	<i>Ca, S, Si, Al, Fe, As, K</i>	<i>Ca, S, Si</i>
PCH04 (yellow)	<i>Ca, S, Si, Al, As, K, Fe</i>	<i>S, As, Si, Ca, K</i>	<i>Ca, S, Si, As</i>
PCH05 (black)	<i>Ca, S, Si, Fe, Al, K</i>	<i>Ca, S, Si, Al</i>	<i>Ca, S, Si</i>
PCH07 (green)	<i>S, Si, Cu, Ca, Al</i>	<i>Ca, S, Si, Cu</i>	<i>Ca, S, Si</i>
PCH08 (red)	<i>Ca, S, Hg, Si, Al, K</i>	<i>Ca, S, Hg</i>	<i>Ca, S, Si</i>
PCH09 (blue)	<i>Ca, S, Si, Al, K</i>	<i>Si, K, As, S, Al, Ca, Co, Fe</i>	<i>Ca, S, Si</i>
PCH10 (dark red)	<i>Ca, S, Si, Al, Na, K, Fe, Mg, P, Cl</i>	<i>Ca, S, Si, Al, K, P</i>	<i>Ca, S, Si</i>

Major elements are marked in italic style

binders [13–15]. These results and the clear separation between the pictorial and the preparation layer point to *a secco* painting technique, which requires a binding medium to attach the pigments onto the wall [16].

The identification of calcium sulfate as the plaster in various mural paintings of colonial churches located on the *Ruta de la Plata* [4, 5] allows us to hypothesize that this may be a typical feature of the wall painting technique in Andean churches.

Pigments

Blue

Two samples (PCH02 and PCH09) of different hues of blue (Table 1) were collected from the wall painting and analyzed by SEM–EDS and micro-Raman spectroscopy. SEM–EDS analysis of the surface of the dark blue sample (PCH02) indicated the presence of Ca, S, Si, and Al with minor amounts of Mg (Table 2). The absence of copper and iron, discarded the presence of the mineral azurite ($2\text{CuCO}_3 \cdot \text{Cu}(\text{OH})_2$) or synthetic Prussian blue ($\text{Fe}_4[\text{Fe}(\text{CN})_6]_3$) as pigments and suggested the use of the organic pigment indigo, in accordance with the Raman spectrum (Fig. 4) of the blue layer in the cross-section, which showed typical bands of indigo at 254, 547, 600, 675, 758, 1128, 1225, 1248, 1311, 1364, 1461, 1483, and 1573 cm^{-1} [17–20], together with a band at 1017 cm^{-1} characteristic of anhydrite [12], presumably from the ground layer. Although the detection of Si and Al in the blue layer may suggest the presence of clay as in the case of maya blue pigment, the bands assigned to indigo in the Raman spectrum do not indicate any bond between the blue dye and the clay [19, 21]. Indigo is a blue dye prepared from the fermentation in water of leaves of plants of the families Papilionaceae, Brassicaceae, and

Polygonaceae [22], which has been extensively used as a pigment and identified in various eighteenth century paintings from South America [4, 5, 23, 24].

Examination by optical microscopy of the cross section of sample PCH09 under polarized light (Fig. 5) revealed blue crystals in the pigment layer. Further analysis by SEM–EDS (Table 2) of this layer indicated silicon, potassium, and arsenic as the main elements together with cobalt. This elemental composition is characteristic of smalt, a blue glass due to the presence of Co^{2+} ions, mostly in tetrahedral coordination, which may contain oxides of Ba, Ca, Na, Mg, Fe, Ni, Cu, and Mn as impurities [25]. The SEM backscatter electron (BSE) image (Fig. 5) revealed particles of different size and morphology, characteristic of smalt. The distribution maps of Si, Co, K, As, and S are in accordance with the presence of smalt particles in the pigment layer of the cross-section. The presence of aluminum and silicon may be ascribed to aluminosilicates while the distribution of calcium and sulfur matches the calcium sulfate layer. The Raman spectrum of the blue layer (not shown) only revealed a band at 1016 cm^{-1} due to anhydrite. This is not surprising because the smalt band at 472 cm^{-1} is often not observed in the Raman spectrum [26]. Smalt was produced in Europe by roasting cobalt minerals to obtain cobalt oxide, which was melted with quartz and potash and poured into cold water to obtain the pigment particles. It has not been produced in the Viceroyalty of Peru so it had to be imported from Europe [27]. As part of our investigations on the chromatic palette of colonial artworks, we have identified smalt in various Andean paintings from the seventeenth and eighteenth centuries [23] and in the Virgin's cloak of the gilded polychrome sculpture of Our Lady of Copacabana in Bolivia [6]. This is the first report of smalt in a wall painting of an Andean church.

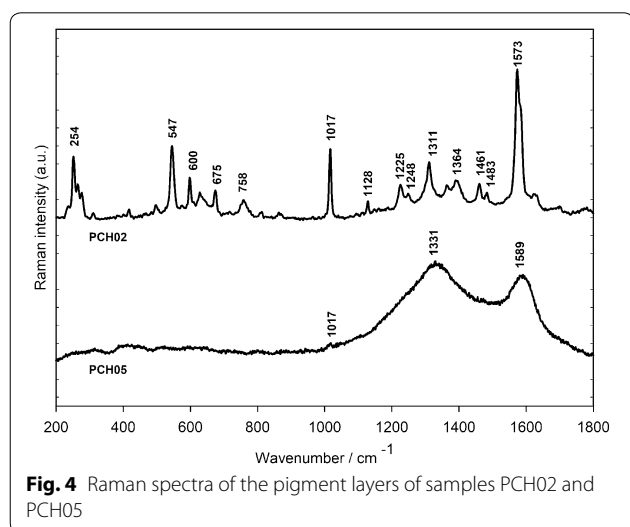


Fig. 4 Raman spectra of the pigment layers of samples PCH02 and PCH05

Black

The Raman spectrum of the surface of sample PCH05 (Fig. 4) indicated a carbon-based pigment due to the presence of two broad bands at 1331 cm^{-1} (D band) and 1589 cm^{-1} (G band) characteristic of amorphous carbon [28]. SEM–EDS analysis of the surface of the sample indicated Ca, S, Si, and Fe as the main elements together with minor amounts of Al and K (Table 2). The FTIR-ATR spectrum of the black pigment layer (not shown) was dominated by characteristic peaks of anhydrite at 1095, 1126, 1149, 672, 611, and 594 cm^{-1} [29] in accordance with a very weak band at 1017 cm^{-1} in the Raman spectrum (Fig. 4). The absence of characteristic hydroxyapatite bands in the infrared spectrum (2012, 599 and 559 cm^{-1}) as well as phosphorous in the EDS micro-analysis discarded the use of a bone black pigment [30].

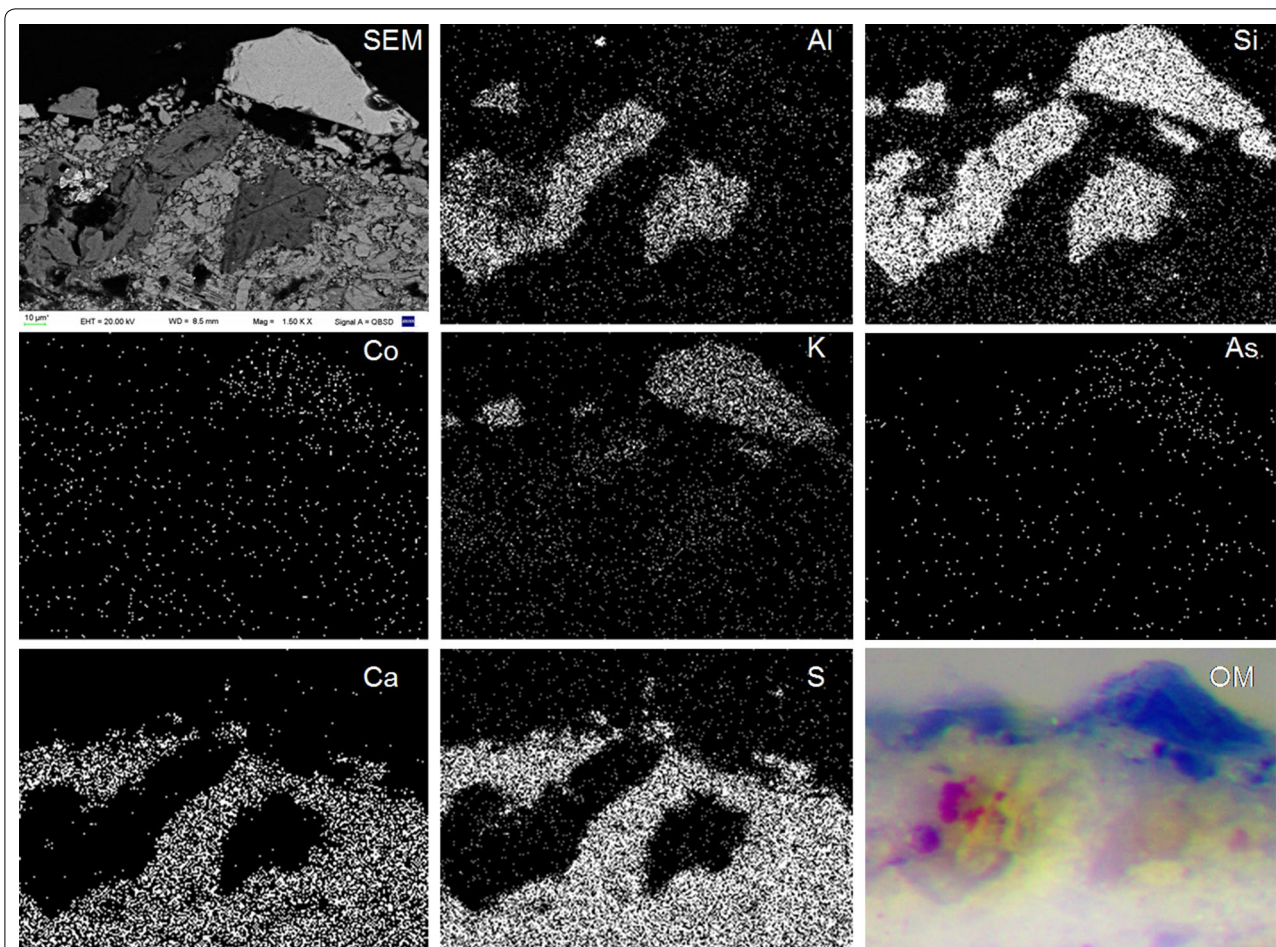


Fig. 5 BSE micrograph of an area of the cross-section of sample PCH09; mapping of Al, Si, Cu, K, As, Ca, and S on the same area; optical image (OM) of an area of the cross-section

These results and comparison with elemental analysis and spectroscopic data of reference samples of carbon-based pigments [28, 30] suggest the application of wood charcoal as the black paint. Recently, we have identified this pigment in a Jesuit sculpture of the eighteenth century [31] and in an Andean mural painting of the church of Copacabana de Andamarca [4].

Yellow

SEM-EDS analysis of the yellow painting layer of sample PCH04 indicated the presence of S and As, with minor amounts of Ca, Si and K (Table 2). This elemental composition together with the yellow color of the sample suggested the presence of orpiment, a highly poisonous arsenic sulfide (As_2S_3). Raman spectrum of the yellow layer on the cross-section (Fig. 6) showed characteristic bands of orpiment at 293, 311, and 355 cm^{-1} [32, 33] together with bands at 1008 and 1017 cm^{-1} ascribed to

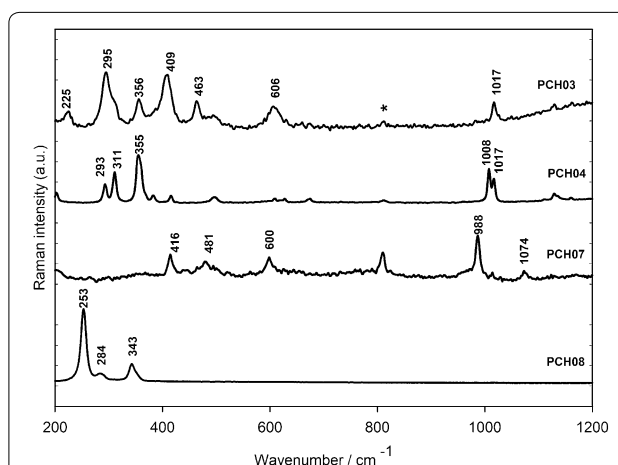


Fig. 6 Raman spectra of the pigment layers of samples PCH03, PCH04, PCH07, and PCH08. Asterisk indicates signal of the poly(methyl methacrylate) resin

gypsum and anhydrite, respectively [12]. Even if orpiment is highly poisonous it was one of the most prized and employed pigments in the Andean colonial palette [34]. It was used as a yellow color or in mixtures with indigo and Prussian blue to obtain different shades of green [24, 34–37]. Orpiment has been detected in most of the illustrations of the seventeenth century manuscript of the Getty Murúa's *Historia General del Piru* [38]. It is worth mentioning that orpiment has been recently found among the funerary objects of a female in an ancient burial site in Chorrillos in Chile [39]. This finding confirms the availability and use of the pigment in the Andean region since pre-Hispanic time.

Orange

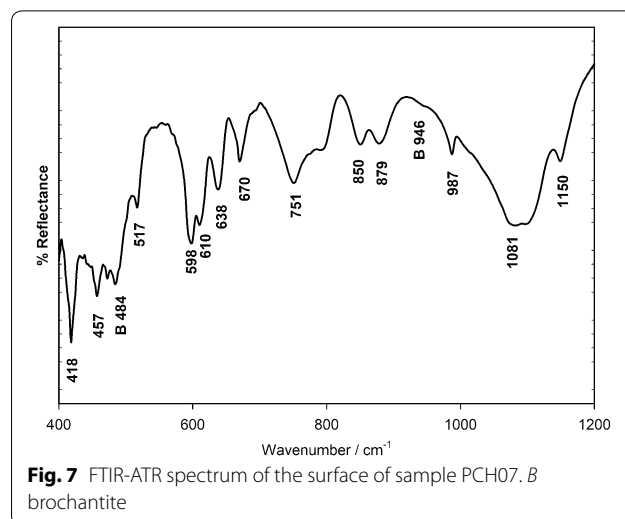
The orange paint in PCH03 was composed by a mixture of orpiment and hematite, in accordance with the elemental composition determined by SEM–EDS (Fe, S, As) (Table 2) and micro-Raman spectroscopy. The Raman spectrum (Fig. 6) of the orange layer showed typical bands of hematite (α -Fe₂O₃) at 225, 295, 409, and 606 cm⁻¹ [40] and a band at 356 cm⁻¹ ascribed to orpiment (As₂S₃) [33]. The broad hematite band at 295 cm⁻¹ overlaps the two characteristic bands of orpiment at 293 and 311 cm⁻¹, which are clearly observed in the Raman spectrum of the yellow pigment in PCH04 (Fig. 6). Further bands at 463 and 1017 cm⁻¹ were assigned to quartz [41] and calcium sulfate, respectively. These results indicate the use of a mixture of hematite and orpiment to obtain the orange hue.

Red earths containing hematite have been identified as pigments in Andean paintings [4, 5, 35–37] and sculptures [7]. Recently, in our investigations on the polychrome of the sculpture of Our Lady of Copacabana in Bolivia we have reported the use of a red bole containing hematite in the gilding of the sculpture [6]. To our knowledge this is the first time that a mixture of hematite with orpiment is used as an orange paint in colonial art.

Green

A copper mineral was assigned as the green pigment in sample PCH07. SEM–EDS results indicated the presence of S, Cu, Ca, and Si (Table 2). The Raman spectrum (Fig. 6) of the green layer revealed an intense band at 988 cm⁻¹ together with bands at 416, 481, 600, and 1074 cm⁻¹ characteristic of antlerite, a basic copper sulfate (Cu₃SO₄(OH)₄) found as a mineral in the Andean mountains in the north of Chile [42–44].

The FTIR-ATR spectrum of the surface of sample PCH07 (Fig. 7) showed characteristic bands of antlerite at 418, 457, 517, 638, 751, 850, 879, 987, and 1150 cm⁻¹. In addition, weak bands of brochantite (Cu₄(SO₄)(OH)₆), a polymorph of antlerite, at 484 and 946 cm⁻¹ were also



observed [44–47]. On the other hand, bands at 598, 610, 670, and 1081 cm⁻¹ are shared by both basic copper sulfates. XRD analysis of the surface of sample PCH07 (Fig. 8) confirmed the presence of crystalline antlerite (peaks at 24.80, 34.94, 42.35, and 44.69) together with quartz.

The SEM–BSE image of an area of the cross-section of sample PCH07 (Fig. 9) revealed particles of irregular size in the pigment layer. The distribution of Cu and S is attributed to the copper sulfate pigment while the distribution of Al and Si may be ascribed to the presence of aluminosilicates, which suggests the mineral origin of the green pigment. Recently, we have identified for the first time the use of antlerite and brochantite as green pigments in samples from a mural painting of an Andean church [4]. This new finding reinforces the use of available minerals in the Andean region as pigments in colonial art following a pre-Hispanic tradition [34, 48, 49].

Red

Two samples extracted of areas of different shades of red color (PCH08 and PCH10) were analyzed by SEM–EDS (Table 2) and Raman microscopy with the aim to identify the red pigments of the mural painting palette. The Raman spectrum (Fig. 6) of the surface of sample PCH08 indicated characteristic bands of mercury sulfide (HgS) at 253, 284, and 343 cm⁻¹ [32]. Vermilion is a synthetic pigment obtained by roasting a mixture of mercury and sulfide while the natural mineral is called cinnabar (α -HgS) [50]. The source of cinnabar in America were the Huancavelica mines in Peru, which were already exhausted in the eighteenth century, but other mines near Guamanga in Peru and in the Quindío Mountains in Colombia were also exploited [51]. Before

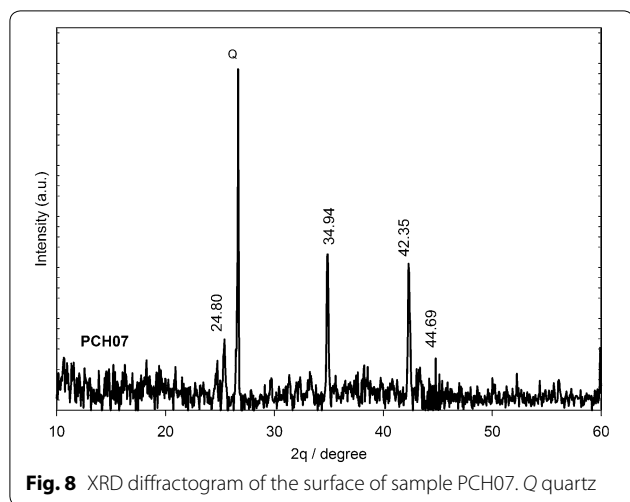


Fig. 8 XRD diffractogram of the surface of sample PCH07. Q quartz

the conquest, the Incas and natives from Peru used cinnabar for painting their faces and bodies, particularly in rituals and sacred ceremonies [34], and there is evidence of the use of cinnabar in mortuary contexts in pre-Columbian times in this region [52, 53]. We have identified this pigment in several colonial paintings [35–37] and polychromated sculptures [41]. In general, analytical studies do not differentiate between cinnabar and vermilion [54], however the presence of impurities that may occasionally be associated with the mineral, indicate a natural origin [55]. Elemental analysis carried out on a crystal of the red layer of the cross-section of PCH08 indicated the presence of Hg, S, and Si, suggesting a natural origin of the pigment in accordance with the availability of the mineral in the region.

The Raman spectrum (not shown) of the surface of sample PCH10 revealed a high fluorescence background and weak bands at 1110, 1245, 1310, 1495, and 1567 cm^{-1} , which suggested the use of carmine, a red lake pigment prepared from carminic acid, the main anthraquinone glucoside in the insect *Dactylopius coccus* Costa [6, 56]. Acid hydrolysis of the red micro-sample to obtain the dye and further analysis by C_{18} HPLC–DAD indicated a peak at 14.25 min in the chromatogram (Fig. 10) whose UV spectrum showed bands at 275 and 495 nm, which matched those of the carminic acid reference and literature data [6].

SEM–EDS analysis of the surface of sample PCH10 indicated the presence of Ca, S, Si, and Al, together with minor amounts of Na, K, Fe, P, Mg, and Cl (Table 2). The identification of sulfur, aluminium, and potassium suggests the use of alum ($\text{KAl}(\text{SO}_4)_2 \cdot 12\text{H}_2\text{O}$) as the mordant applied in the preparation of the red lake. In European historical recipes, this salt was most

commonly used as a reagent to form the substrate for the dyestuff [57]. On the other hand, elements such as P, S, K, Mg, and Cl detected in the cochineal insects have been identified in red lakes in paintings [57]. The presence of P, Mg, and Cl in sample PCH10 points to a contribution of the dyestuff raw material to the lake.

Cochineal has been used as a textile dye since pre-Inca times and as a pigment and glaze in some colonial paintings from the seventeenth and eighteenth centuries [58]. Our finding adds new information on the use of the lake of carminic acid as a pigment in a colonial mural painting.

Organic binders and painting technique

Based on the observation of Raman bands attributed to degraded organic binders in various of the micro samples (Fig. 3) and considering the hypothesis of *a secco* painting technique, we selected four samples (PCH02, PCH04, PCH05, and PCH08) of the mural painting and submitted them to extraction with ammonia, using a modification of the procedure reported in [8] and described in the Experimental section. After separation of the lipid fraction from the proteins, both fractions were derivatised and analyzed by GC–MS. Fatty acids obtained by saponification and further acidification were analyzed as their methyl esters (FAME) while sterols were derivatised as their trimethylsilyl derivatives (TMS). The chromatograms of the four samples showed a major presence of palmitic (C16:0) and stearic (C18:0) acids, together with minor amounts of myristic acid (C14:0) in samples PCH02 and PCH05, and oleic acid (C18:1) in samples PCH04 and PCH05. Samples PCH05 and PCH08 also showed azelaic (nonanedioic) acid, a degradation product of C-18 polyunsaturated fatty acids in siccative oils such as linseed oil. The ratio between the areas of the FAME of palmitic and stearic acids (P/S) is a parameter that gives information on the lipid source based on the stability of both saturated fatty acids [59]. Samples PCH02 and PCH05 showed P/S ratios of 1.2 while PCH04 and PCH08 gave ratios of 0.9 and 1.4, respectively. These values are close to those reported previously for a naturally aged model sample of linseed oil applied on gypsum (1.6) compared to a model sample of whole egg on gypsum (2.8) [4]. Moreover, the ratio of the areas of azelaic and palmitic acids (A/P) is a parameter that helps in the determination of a siccative oil due to the presence of reactive linoleic and linolenic acids in comparison to egg, which is rich in oleic acid [59]. Samples PCH05 and PCH08 showed A/P values of 0.1 and 0.2 close to that of a model sample of linseed oil on gypsum (0.1) [4] while azelaic acid was absent in samples PCH02 and PCH04. Three of the samples (PCH02, PCH05, and PCH08)

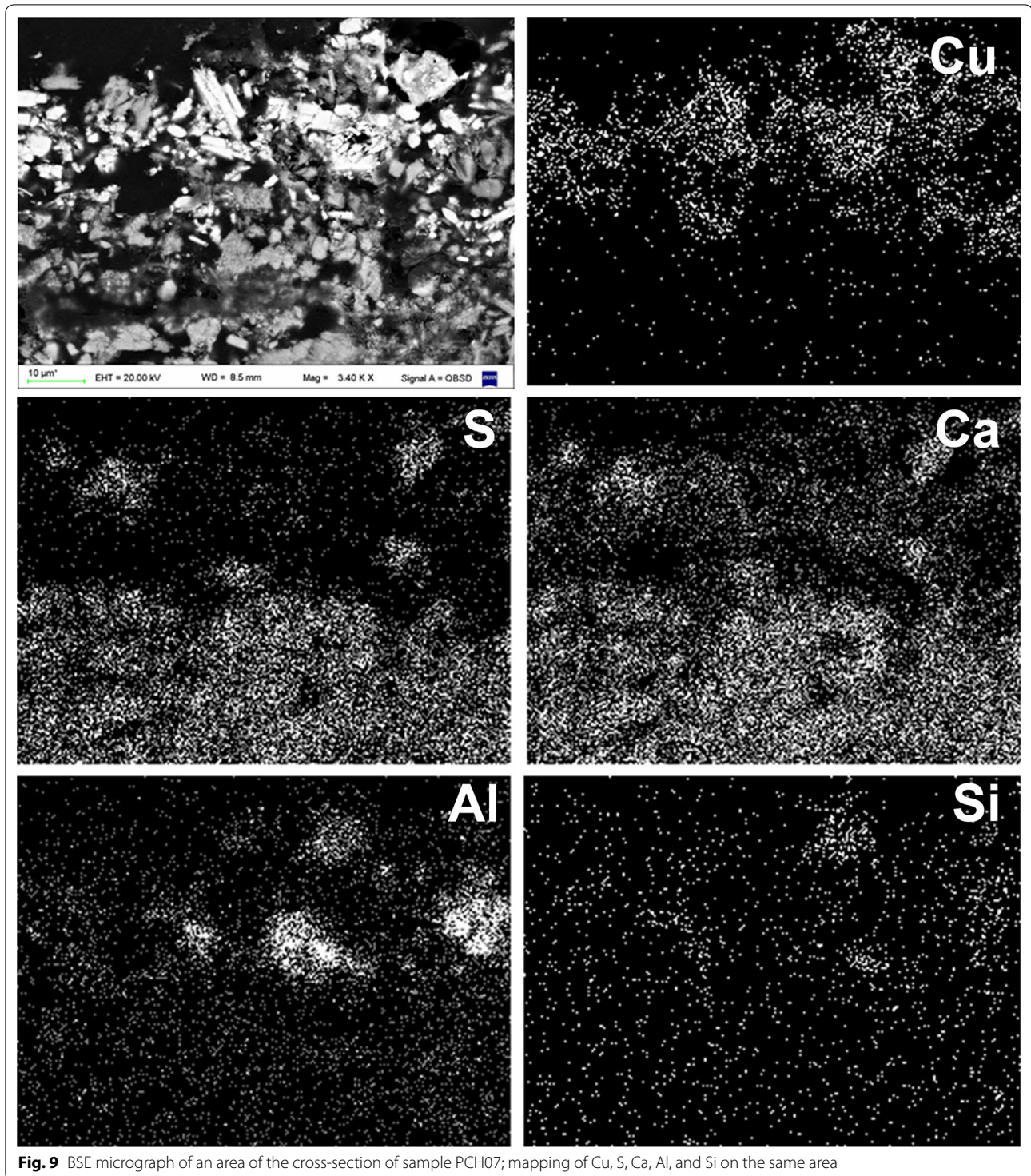


Fig. 9 BSE micrograph of an area of the cross-section of sample PCH07; mapping of Cu, S, Ca, Al, and Si on the same area

showed the presence of cholesterol, which indicates the use of egg as a binder. The identification of a mixture of egg and a siccative oil in samples PCH05 and PCH08 points to a tempera grassa [16].

Protein identification in samples PCH02, PCH04, and PCH08 was not possible due to the presence of only traces of a few amino acids. On the contrary, sample PCH05 showed an amino acid composition very close to that of the mock up of whole egg and animal glue on

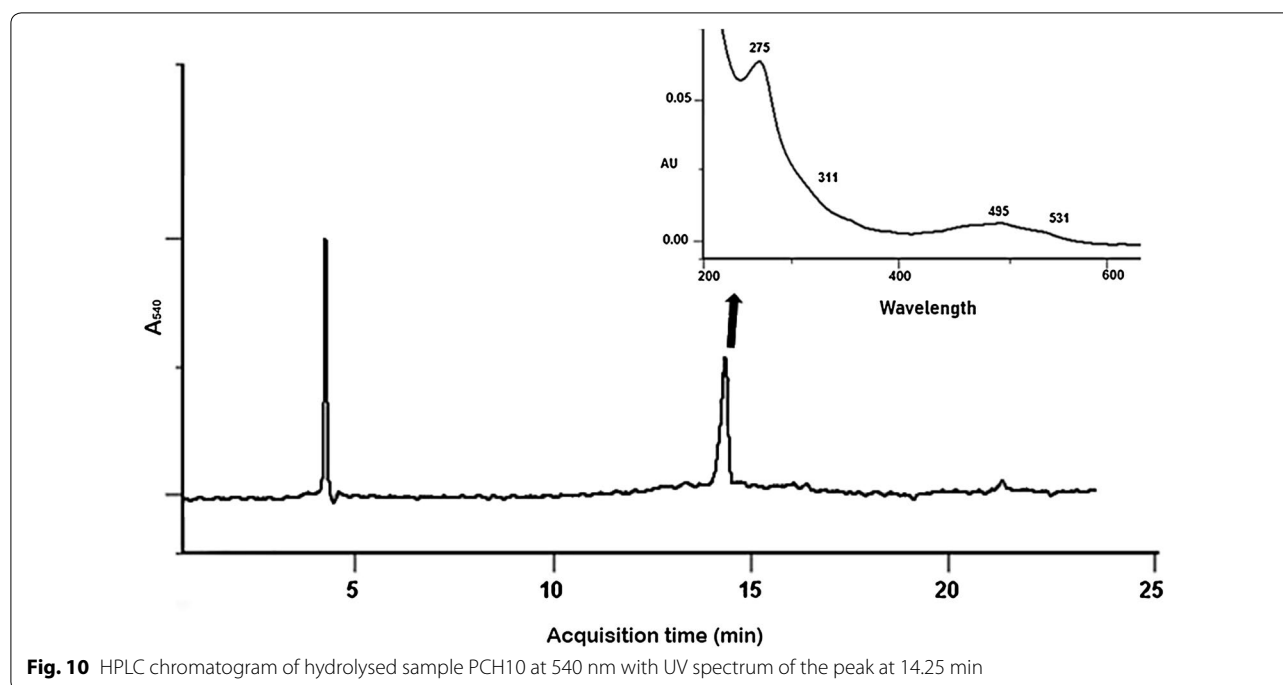


Fig. 10 HPLC chromatogram of hydrolysed sample PCH10 at 540 nm with UV spectrum of the peak at 14.25 min

Table 3 Relative amino acid percentage content of sample PCH05 and model sample of animal glue and whole egg on gypsum

Sample	Ala	Gly	Thr	Ser	Val	Leu	Ile	Pro	Hyp	Asp	Glu	Phe	Lys
PCH-05	1.5	8.4	2.4	10.6	1.3	5.0	1.0	8.7	6.8	10.8	19.5	12.8	11.2
Model sample	2.8	7.0	3.4	5.5	3.3	10.8	2.4	10.4	5.0	10.9	17.7	10.2	10.6

gypsum (Table 3). The use of animal glue was inferred from the high proportion of glycine (Gly) and the presence of hydroxyproline (Hyp) (a marker of animal glue, which is absent in egg). The relatively high amounts of aspartic acid (Asp), serine (Ser), and glutamic acid (Glu) indicate the use of egg, which has previously been determined from the identification of cholesterol in the neutral fraction of PCH05 [60]. These results suggest the use of a mixture of egg and a siccative oil as the pigment binder and the application of the paints onto a gypsum preparation layer presumably primed with an animal glue, as Pacheco's painting treatise recommends for *a secco* technique [16]. Currently, we are applying proteomic tools and mass spectrometry techniques to identify more accurately the proteinaceous binders, particularly in those samples that showed only traces of amino acids.

Conclusions

The use of a combination of analytical techniques (SEM-EDS, micro-Raman spectroscopy, FTIR-ATR, XRD, HPLC-DAD, and GC-MS) allowed us to characterize the

pigments and binders as well as the painting technique in a mural painting of the eighteenth century church of San Andrés de Pachama in northern Chile. The painting palette comprises orpiment, vermilion, indigo, smalt, antlerite, hematite, a carmine lake, and a carbon-based black pigment. Antlerite, a copper sulfate hydroxide, is an uncommon pigment in the colonial palette and has previously been identified only in mural paintings in two colonial churches in Bolivia [4, 5]. Its identification in paints applied on masks that were found in an archeological site in the Tarapacá region in Chile reinforces its use as a pigment since pre-Hispanic times [48, 49]. The analytical results indicate *a secco* technique with the use of a mixture of linseed oil and egg as pigment binders. This study contributes to our knowledge on the Colonial chromatic palette, highlighting the use of smalt and particularly the precious cochineal lake as pigments in mural painting. At the same time, it significantly expands our understanding of the original painting technique in mural paintings from Andean churches near the *Ruta de la Plata*, during historical times.

Authors' contributions

MSM, EPT, and MS coordinated the study and prepared the draft manuscript. EPT performed the FT-IR and SEM-EDS analyses and interpreted the Raman spectra of the cross-sections of the samples. SG contributed portable FRX analysis and JC performed the Raman microscopy analyses on the surface of the samples. DMCR performed the lipid and protein analysis and VC performed the HPLC-DAD analysis of the carmine lake sample. CRL extracted the samples from the mural painting. EPT, JC, SG, and MSM carried out the interpretation of the analytical results. GS, MP, and FG selected the mural painting and contributed the historical background of the research. All authors read and approved the final manuscript.

Author details

¹ CONICET-Universidad de Buenos Aires, Unidad de Microanálisis y Métodos Físicos en Química Orgánica (UMYFOR), Pabellón 2, Ciudad Universitaria, C1428EGA Ciudad Autónoma de Buenos Aires, Argentina. ² CONICET, Godoy Cruz 2290, C1425FQB Ciudad Autónoma de Buenos Aires, Argentina. ³ Instituto de Alta Investigación, Laboratorio de Análisis e Investigaciones Arqueométricas, Universidad de Tarapacá, Casilla-6D, Arica, Chile. ⁴ Ministerio de Culturas y Turismo, Taller de Conservación y Restauración del Patrimonio Mueble, La Paz, Bolivia. ⁵ UMR 8096 ArchAm (CNRS-Paris1), Nanterre, France. ⁶ Centro de Estudios del Patrimonio, Universidad Adolfo Ibáñez, Santiago, Chile. ⁷ Fundación Altiplano Monseñor Salas Valdés, Andrés Bello 1515, Arica, Chile. ⁸ Centro de Investigación en Arte, Materia y Cultura, IIAC, Universidad Nacional de Tres de Febrero, Avda. Antártida Argentina 1355, C1104ACA Ciudad Autónoma de Buenos Aires, Argentina.

Acknowledgements

The authors are indebted to the Consejo Nacional de Investigaciones Científicas y Técnicas (CONICET) (11220130100288CO), Agencia Nacional de Promoción Científica y Tecnológica (ANPCyT) (PICT 2016-0349), the University of Buenos Aires (20020170100340BA and 20020130300010BA), Argentina, and the Consejo Nacional de Investigación Científica y Tecnológica del Estado de Chile (FONDECYT 1150974) for the financial support. D.C.M.R. thanks CONICET for a Doctoral Fellowship; E.T., G.S., V.C., and M.S.M. are Research Members of CONICET. The authors would like to thank Doly Chemes and Dr. Rosa María Álvarez (Laboratorio de Espectroscopia Raman, INQUINOA-CONICET, Universidad de Tucumán, Argentina) for performing the Raman spectra of the cross-sections of the samples and to Dr. María Cecilia Fuertes for XRD analysis. We also wish to thank to Convenio de Desempeño UTA-MINEDUC for its support to the Laboratorio de Análisis e Investigaciones Arqueométricas from the Universidad de Tarapacá.

Competing interests

The authors declare that they have no competing interests.

Availability of data and materials

Not applicable.

Publisher's Note

Springer Nature remains neutral with regard to jurisdictional claims in published maps and institutional affiliations.

Received: 19 July 2018 Accepted: 12 October 2018

Published online: 19 October 2018

References

- Fundación Altiplano. Iglesias andinas de Arica y Parinacota: las huellas de la Ruta de la Plata. Arica: QuadGraphics; 2012.
- Choque Mariño C, Muñoz Ovalle I. El Camino Real de la Plata. Circulación de mercancías e interacciones culturales en los valles y altos de Arica (siglos XVI al XVIII). *Historia*. 2016;49:57–86.
- Guzmán F, Maier M, Pereira M, Sepúlveda M, Siracusano G, Cárcamo J, Castellanos D, Gutiérrez S, Tomasini E, Corti P, Rúa C. Programa iconográfico y material en las pinturas murales de la iglesia de San Andrés de Pachama, Chile. *Colon Latin Am Rev*. 2016;25:245–64.
- Tomasini E, Rodríguez DC, Gómez B, de Faria DLA, Rúa Landa C, Siracusano G, Maier MS. A multi-analytical investigation of the materials and painting technique of a wall painting from the church of Copacabana de Andamarca (Bolivia). *Microchem J*. 2016;128:172–80.
- Rúa C, Sepúlveda M, Gutiérrez S, Cárcamo-Vega JJ, Surco-Luque J, Campos-Vallette M, Guzmán F, Conti P, Pereira M. Raman identification of pigments in wall paintings of the Colonial period from Bolivian churches in the Ruta de La Plata. *Conserv Sci Cult Herit*. 2017;17:117–35.
- Tomasini EP, Marte F, Careaga VP, Rúa Landa C, Siracusano G, Maier MS. Virtuuous colors for Mary. Identification of lapis lazuli, smalt and cochineal in the Andean colonial image of Our Lady of Copacabana (Bolivia). *Philos Trans Royal Soc A*. 2016;374:20160047.
- Gómez BA, Parera SD, Siracusano G, Maier MS. Integrated analytical techniques for the characterization of painting materials in two South American polychrome sculptures. *e-Preserv Sci*. 2010;7:1–7.
- Andreotti A, Bonaduce I, Colombini MP, Gautier G, Modugno F, Ribechini E. Combined GC/MS analytical procedure for the characterization of glycerolipid, waxy, resinous, and proteinaceous materials in a unique paint microsample. *Anal Chem*. 2006;78:4490–500.
- Careaga VP, Muniain C, Maier MS. Fatty acid composition of the edible sea cucumber *Athyonium chilensis*. *Nat Prod Res*. 2013;27:639–47.
- Lantos I, Spangenberg JE, Giovannetti MA, Ratto N, Maier MS. Maize consumption in pre-Hispanic south-central Andes: chemical and microscopic evidence from organic residues in archaeological pottery from western Tinogasta (Catamarca, Argentina). *J Archaeol Sci*. 2015;55:83–99.
- Bersani D, Lottici PP, Casoli A, Cauzzi D. Pigments and binders in "Madonna con Bambino e S. Giovannino" by Boticelli investigated by micro-Raman and GC/MS. *J Cult Herit*. 2008;9:97–102.
- Prieto-Taboada N, Gómez-Laserna O, Martínez-Arkarazo I, Olazabal MA, Madariaga JM. Raman spectra of the different phases in the CaSO₄-H₂O system. *Anal Chem*. 2014;86:10131–7.
- Nevin A, Osticioli I, Anglos D, Burnstock A, Cather S, Castellucci E. Raman spectra of proteinaceous materials used in paintings: a multivariate analytical approach for classification and identification. *Anal Chem*. 2007;79:6143–51.
- Osticioli I, Nevin A, Anglos D, Burnstock A, Cather S, Becucci M, Fotakis C, Castellucci E. Micro-Raman and fluorescence spectroscopy for the assessment of the effects of the exposure to light on films of egg white and egg yolk. *J Raman Spectrosc*. 2008;39:307–13.
- Manzano E, García-Atero J, Domínguez-Vidal A, Ayora-Cañada MJ, Capitán-Valley LF, Navas N. Discrimination of aged mixtures of lipidic paint binders by Raman spectroscopy and chemometrics. *J Raman Spectrosc*. 2012;43:781–6.
- Pacheco F. *Arte de la pintura*. 2nd ed. Barcelona: Las Ediciones de Arte; 1982.
- Tatsch E, Schrader B. Near-infrared Fourier transform Raman spectroscopy of indigoids. *J Raman Spectrosc*. 1995;26:467–73.
- Burgio L, Clark RJH. Library of FT-Raman spectra of pigments, minerals, pigment media and varnishes, and supplement to existing library of Raman spectra of pigments with visible excitation. *Spectrochim Acta A*. 2001;57:1491–521.
- Sanchez del Rio M, Picquart M, Haro-Poniatowski E, van Elslande E, Hugo Uc V. On the Raman spectrum of Maya blue. *J Raman Spectrosc*. 2006;37:1046–53.
- Baran A, Fiedler A, Schulz H, Baranska M. In situ Raman and IR spectroscopic analysis of indigo dye. *Anal Methods*. 2010;2:1372–6.
- Doménech A, Doménech-Carbó MT, Edwards HGM. On the interpretation of the Raman spectra of Maya Blue: a review on the literature data. *J Raman Spectrosc*. 2011;42:86–96.
- Schweppe H. Indigo and woad. In: FitzHugh EW, editor. *Artists' pigments*, vol. 3. Washington DC: National Gallery of Art; 1997. p. 81–107.
- Seldes AM, Burucúa JE, Maier MS, Abad G, Jáuregui A, Siracusano G. Blue pigments in South American painting (1610–1780). *J Am Inst Conserv*. 1999;38:100–23.
- Marte F, Careaga VP, Mastrangelo N, de Faria DLA, Maier MS. The Sibyls from the church of San Pedro Telmo: a micro-Raman spectroscopic investigation. *J Raman Spectrosc*. 2014;45:1046–51.
- Muhlethaler B, Thissen J. Smalt. In: Roy A, editor. *Artists' pigments*, vol. 2. Oxford: Oxford University Press; 1993. p. 113–30.
- Robinet L, Spring M, Pagès-Camagna S. Vibrational spectroscopy correlated with elemental analysis for the investigation of smalt pigment and its alteration in paintings. *Anal Methods*. 2013;5:4628–38.

27. Bargalló M. La minería y la metalurgia en la América española durante la época colonial. Ciudad de México: Fondo de cultura económica; 1955.
28. Tomasini EP, Halac EB, Reinoso M, Di Liscia EJ, Maier MS. Micro-Raman spectroscopy of carbon-based black pigments. *J Raman Spectrosc.* 2012;43:1671–5.
29. Bishop JL, Lane MD, Dyar MD, King SJ, Brown AJ, Swayze GA. Spectral properties of Ca-sulfates: gypsum, bassanite, and anhydrite. *Am Mineral.* 2014;99:2105–15.
30. Tomasini E, Siracusano G, Maier MS. Spectroscopic, morphological and chemical characterization of historic pigments based on carbon. Paths for the identification of an artistic pigment. *Microchem J.* 2012;102:28–37.
31. Tomasini EP, Gómez B, Halac EB, Reinoso M, Di Liscia EJ, Siracusano G, Maier MS. Identification of carbon-based black pigments in four South American polychrome wooden sculptures by Raman microscopy. *Herit Sci.* 2015;3:19.
32. Frost RL, Martens WN, Kloprogge JT. Raman spectroscopic study of cinnabar (HgS), realgar (As₂S₃), and orpiment (As₂S₃) at 298 and 77 K. *N Jahrb Miner Monatshefte.* 2002;10:469–80.
33. Forneris R. The infrared and raman spectra of realgar and orpiment. *Am Mineral.* 1969;54:1062–4.
34. Siracusano G. Pigments and powers in the Andes: from the material to the symbolic in Andean cultural practices 1500–1800. London: Archetype Publications; 2011.
35. Seldes AM, Burucúa JE, Siracusano G, Maier MS, Abad G. Green, yellow and red pigments in the South American painting (1610–1780). *J Am Inst Conserv.* 2002;41:225–42.
36. Maier M, Gómez B, Parera SD. Análisis científico de los materiales pictóricos. In: Siracusano G, editor. La paleta del espanto. Color y cultura en los cielos e infiernos de la pintura colonial andina. Buenos Aires: UNSAM Edita; 2010. p. 85–95.
37. Seldes A, Abad G, Maier MS. Composición química de las capas de pintura. Una serie de pinturas cuzqueñas de Santa Catalina: historia, restauración y química. Buenos Aires: Fundación Tarea; 1998. p. 37–52.
38. Phipps E, Turner N, Trentelman K. In: Cummins TBF, Anderson B, editors. The Getty Murúa: essays on the making of Martín de Murúa's "Historia General del Piru". Los Angeles: The Getty Research Institute; 2010. p. 125–41.
39. Ogalde JP, Salas CO, Lara N, Leyton P, Paipa C, Campos-Vallette M, Arriaza B. Multi-instrumental identification of orpiment in archaeological mortuary contexts. *J Chilean Chem Soc.* 2014;59:2571–3.
40. de Faria DLA, Silva SV, de Oliveira MT. Raman microspectroscopy of some iron oxides and oxyhydroxides. *J Raman Spectrosc.* 1997;28:873–8.
41. Kingman K, Hemley R. Raman spectroscopic study of microcrystalline silica. *Am Mineral.* 1994;79:269–73.
42. Bouchard M, Smith DC. Catalogue of 45 reference Raman spectra of minerals concerning research in art history or archaeology, especially on corroded metals and coloured glass. *Spectrochim Acta A.* 2003;59:2247–66.
43. Frost R. Raman spectroscopy of selected copper minerals of significance in corrosion. *Spectrochim Acta A.* 2003;59:1195–204.
44. Gilbert B, Denoël S, Weber G, Allart D. Analysis of green copper pigments in illuminated manuscripts by micro-Raman spectroscopy. *Analyst.* 2003;128:1213–7.
45. van der Marel HW, Beutelspacher H. Atlas of infrared spectroscopy of clay minerals and their admixtures. Amsterdam: Elsevier; 1976.
46. Lane MD. Mid-infrared emission spectroscopy of sulfate and sulfate-bearing minerals. *Am Mineral.* 2007;92:1–18.
47. Makreski P, Jovanovski G, Dimitrovska S. Minerals from Macedonia XIV. Identification of some sulfate minerals by vibrational (infrared and Raman) spectroscopy. *Vib Spectrosc.* 2005;39:229–39.
48. Sepúlveda M, Figueroa V, Pages S. Copper pigment-making in the Atacama Desert (Northern Chile). *Latin Am Antiq.* 2013;24:467–82.
49. Sepúlveda M, Figueroa V, Cárcamo J. Pigmentos y pinturas de mineral de cobre en la región de Tarapacá, norte de Chile: nuevos datos para una tecnología pigmentaria prehispánica. *Estudios Atacameños.* 2014;48:23–37.
50. Gettens RJ, Feller RL, Chase WT. In: Roy A, editor. Artists' pigments, vol. 2. Oxford: Oxford University Press; 1993. p. 159–82.
51. Burger RL, Lane KE, Cooke CA. Ecuadorian cinnabar and the prehispanic trade in vermilion pigment: viable hypothesis or red herring. *Latin Am Antiq.* 2016;27:23–35.
52. Cesareo R, Bustamante A, Fabian J, Calza C, Dos Anjos M, Lopes RT, Elera C, Shimada I, Curayd V, Rizzutto MA. Energy-dispersive X-ray fluorescence analysis of a pre-Columbian funerary gold mask from the Museum of Sicán, Peru. *X-ray Spectrom.* 2010;39:122–6.
53. Galli A, Bonizzoni L, Sibilia E, Martini M. EDXRF analysis of metal artifacts from the grave goods of the Royal Tomb 14 of Sipán, Peru. *X-ray Spectrom.* 2011;40:74–8.
54. Gettens RJ, Feller RL, Chase WT. Vermilion and cinnabar. *Stud Conserv.* 1972;17:45–69.
55. Nöller R. Cinnabar reviewed: characterization of the red pigment and its reactions. *Stud Conserv.* 2015;60:79–87.
56. Svobodova E, Bosakova Z, Ohlidalova M, Novotna M, Nemeč I. The use of infrared and Raman microspectroscopy for identification of selected red organic dyes in model color layers of works of art. *Vib Spectrosc.* 2012;63:380–9.
57. Kirby J, Spring M, Higgitt C. The technology of red lake pigment manufacture: study of the dyestuff substrate. *Natl Gallery Tech Bull.* 2005;26:71–87.
58. Siracusano G, Maier MS. More reddish than grain. Cochineal in colonial andean painting. A red like no other: how cochineal colored the world. The Museum of International Folk Art (MOIFA): Santa Fe; 2015. p. 212–9.
59. Mills JS, White R. The organic chemistry of museum objects. Oxford: Butterworth-Heinemann; 1994.
60. Gautier G, Colombini MP. GC-MS identification of proteins in wall painting samples: a fast clean-up procedure to remove copper-based pigment interferences. *Talanta.* 2007;73:95–102.

Submit your manuscript to a SpringerOpen[®] journal and benefit from:

- Convenient online submission
- Rigorous peer review
- Open access: articles freely available online
- High visibility within the field
- Retaining the copyright to your article

Submit your next manuscript at ► springeropen.com